

Power Line Impedance Characterization of Automotive Loads at the Power Line Communication Frequency Range

Marc Aragón, Mauricio Salinas, Pere J. Riu and Ferran Silva

Grup de Compatibilitat Electromagnètica (GCEM) Departament d'Enginyeria Electrònica (DEE)
Universitat Politècnica de Catalunya (UPC),
Barcelona, Spain

Abstract— A complete system able to measure complex impedance, both in magnitude and phase, of an automotive electrical load is designed. The development of such system emerged from the need of measure the impedance of these loads in a wide range of frequencies (100 kHz to 30 MHz) while being connected to power supply and in operation. This powered up condition introduces several problems when the impedance is measured by means of traditional instruments such as Vector Network Analyzers (VNA), which could be damaged by transients. Understanding the behaviour of electrical cars loads in the frequency domain is of primary importance not only for in-vehicle Power Line Communication (PLC) channels response, but also to understand electromagnetic emissions (EMI) problems related with this type of communications.

Keywords- PLC, power lines; impedance measurements, automotive systems.

I. INTRODUCTION

Power Line Communication interest has increased in the last years and they are now in full expansion. In automotive applications, it is intended to be used in the high frequency range, called broadband, from 1 MHz to 30 MHz. This one is also known as BPL (Broadband over Power Lines) and it is compatible with the future in-car multimedia applications, which are focused on high-speed communication (suitable for SAE class D networks [1]).

Different transmission parameters (like noise, attenuation or impedance) of the power line channel have been evaluated in several publications. Therefore, there are some interesting solutions for indoor power line networks with advanced transmission techniques. We can mention an example of these studies [2], where mains properties of the channel are analyzed and the effects of load impedance, line length, and branches on such systems are described. However, most of them are still based on in-house networks environment, and only a few recent publications help us to better model and understand the PLC on the automotive network. For example, the studies [3] and [4] are focused on car network noise environment, in [5] and [6] an initial channel response analysis of the car harness is presented and discussed, with a considerable number of channel measurements that have been made in a two different

commercial cars. Finally, the functionality of two different PLC standards for in-vehicle networks are evaluated in [7].

In a similar way, from an electromagnetic point of view, the behaviour of PLC in automotive environment it is not enough evaluated as it has been done in the in-house PLC applications [8] and [9]. And, obviously, in the automotive scenario the power supply layout and the equipments connected differ very much from the indoor ones. This paper is dedicated to improve the knowledge of the in-vehicle power lines communications by means of the evaluation of the automotive loads impedance at the PLC frequency range. As it is expected, every load connected to the power network will have certain effect on the line, thus creating the need of precisely knowing this impedance to calculate the transfer function of the transmission line. But also, understanding the behaviour of electrical loads in the frequency domain is of primary importance for EMC problems [10] and [11], and therefore is useful for evaluate electromagnetic interferences (EMI) related with in-vehicle power lines networks.

In this paper, a measurement method is developed to obtain both, loads impedance magnitude and phase, in the whole frequency range (0.1 up to 30 MHz). First, we analyze their behaviour from a functional point of view, and later we obtain their impedance response related with the electromagnetic compatibility of the system. To address those issues loads have been modelled by three impedances, one in differential mode, Z_d , between battery positive and negative lines, and two in common mode (Z_{C2} between battery positive line and chassis car, Z_{C3} between battery negative line and chassis car).

II. SYSTEM DEVELOPMENT

Due to high level transients produced by car's loads during their normal function, is not recommendable to make measurements at upper frequencies than 1 MHz with high sensitivity instrumentation, because it could be damaged. For example, during the connection or disconnection of the DC motors power supply, current standards, like ISO 7637-2 [12], indicate that transients up to 100 V can be easily generated. We also have to consider the noise on the loads generated by their own operation because it introduces an error during the

This work was sponsored in part by the Spanish research project MICINN (DPI2007-63878).

measurements [13]. All these restrictions were considered in order to develop the new method.

We present a method which gets voltage (V) and current (I) in both, magnitude and phase, through direct measurements of the loads. Then Ohm's law is used in order to determine the resulting impedance Z of any given Device Under Test (DUT). Fig. 1 displays a fine first-sight diagram to understand the principle of functioning.

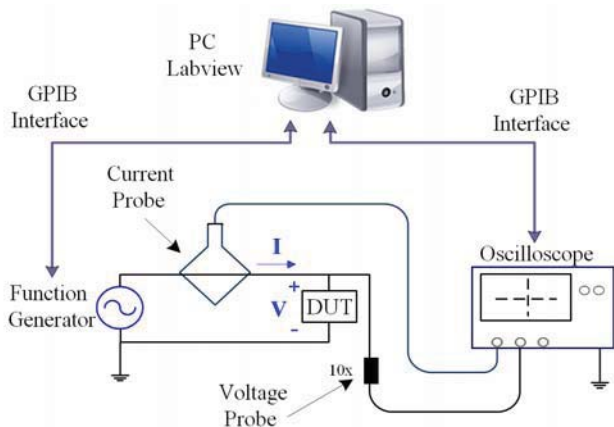


Figure 1. Basic system schematic.

This method is based on a function generator which is AC coupled to the terminals of the DUT. Simultaneously, an oscilloscope acquires, in magnitude and phase, the resulting voltage and current. Making all these measures and impedance calculations manually would result in an excessive time consuming and tedious task. The solution to this issue is to automate the data acquisition by a controller system employing a Personal Computer (PC) running LabVIEW. The developed control software actuates on the configuration of the function generator and the oscilloscope. GPIB interface was employed to communicate these instruments with the PC. The software

running on the PC sets the AC waveform on the function generator and acquires the data from the oscilloscope which is stored, repeating this process for each frequency. This process of calculating Z from the measurements is performed as many times as frequency steps are desired, therefore, frequency vs. impedance or phase graphics are obtained and plotted.

Fig. 2 shows the complete measurement setup, the following description explains the different devices functions from left to right. The function generator (Hameg HM8134) stimulates, in a frequency sweep mode, the load to characterize. A common mode choke is inserted between the function generator and the rest of the system to decrease the common mode current which will produce a measurement error. Because the choke does not work properly at lower frequencies, a balun (RF Transformer T1-1-X65+), is used to cover these ranges of frequencies; it also converts the unbalanced signal produced by the function generator to the balanced one applied to the DUT. Next, a set of jumpers are placed in order to choose among three different kinds of measurements. This provides the ability to measure, not only the differential impedance (Z_d) between the DUT terminals, but also the common mode impedances (Z_{C2} and Z_{C3}) between each terminal and ground. A couple of the serial capacitors are inserted to stop DC power from damaging the output of the function generator. In order to ensure the measurement reproducibility the described setup is made by means of a printed circuit board (PCB).

Next devices are two passive oscilloscope voltage probes (Tektronix P6139A), which measure the signal present at the positive and negative terminals. This means that the final Z_d value is calculated by subtraction of the two measurements. This procedure reduces the associate error. On the other hand, Z_{C2} and Z_{C3} are measured only by one voltage probe, referred to the instruments ground.

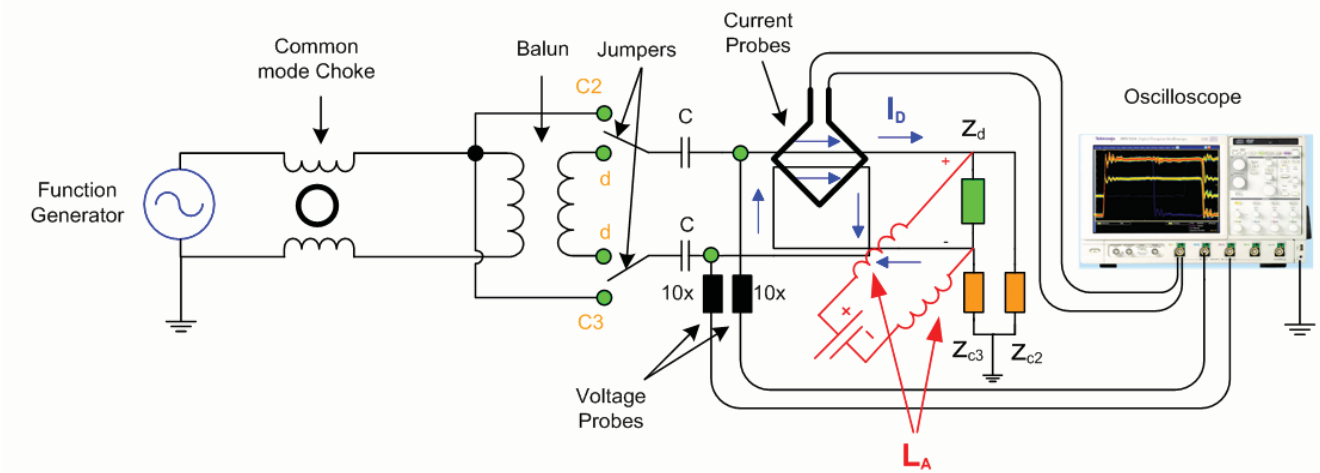


Figure 2. Complete system schematic.

In order to determine the current flowing in the forward and return conductors, a current probe (Solar Electronics 9123-1N) is used as shown in Fig. 2. That means that during Z_d evaluation, the differential current is measured twice, while the magnetic fields produced by the common mode current are cancelled each other in the probe. When measuring the common mode Z_{C2} or Z_{C3} , the current probe is located only in the correspondent going ahead wire and, therefore, only the corresponding common mode current of interest is measured. Employing all these probes, an Oscilloscope (Tektronix DPO7104) can be used without risk of instrument damage.

Finally, we have to consider the connection of the automotive loads under study to the battery power supply. A DC power source is connected to the DUT terminals through a pair of inductors (L_A) in order to power up the device. Those inductors ensure that a most of the RF signal is directed to the DUT and is not dissipated at the power source, which usually has output impedance lower than the one we want to measure. It is necessary to use different types of inductors in order to obtain a good response in the wide frequency range of interest.

As it can be seen in Fig. 2, all three impedances of interest are in fact connected in a "delta" configuration, making it virtually impossible to measure each one independently. Therefore each measurement performed on any DUT will record a value of impedance equal to the impedance of interest in parallel with the series of the other two; these measures are here designated with the names Z_1 , Z_2 and Z_3 . Fig. 3 illustrates this configuration more clearly.

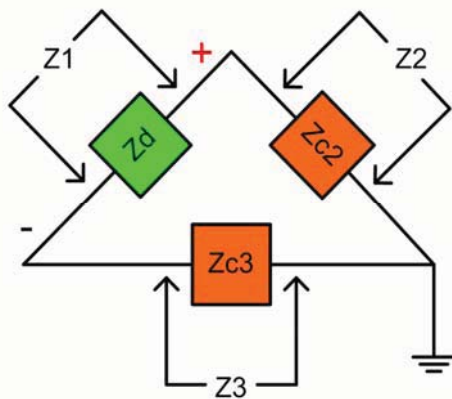


Figure 3. Impedance Configuration.

Once these three impedances values are measured, impedances Z_d , Z_{C2} and Z_{C3} are then calculated in a Matlab. The numerical equations used are shown in (1), (2) and (3).

$$Z_d = \frac{1}{2} \cdot \frac{Z_1^2 - 2 \cdot Z_3 \cdot Z_1 - 2 \cdot Z_2 \cdot Z_1 - 2 \cdot Z_3 \cdot Z_2 + Z_3^2 + Z_2^2}{Z_1 - Z_2 - Z_3} \quad (1)$$

$$Z_{c2} = -\frac{1}{2} \cdot \frac{Z_1^2 - 2 \cdot Z_3 \cdot Z_1 - 2 \cdot Z_2 \cdot Z_1 - 2 \cdot Z_3 \cdot Z_2 + Z_3^2 + Z_2^2}{Z_3 - Z_2 + Z_1} \quad (2)$$

$$Z_{c3} = -\frac{1}{2} \cdot \frac{Z_1^2 - 2 \cdot Z_3 \cdot Z_1 - 2 \cdot Z_2 \cdot Z_1 - 2 \cdot Z_3 \cdot Z_2 + Z_3^2 + Z_2^2}{Z_1 - Z_3 + Z_2} \quad (3)$$

These expressions were obtained by means of math-processor MAPLE.

III. MEASUREMENT ERROR

It is a known fact that the action of measuring a quantity, which ever this is, inherently introduces an error, this system is no exception. Prior to conduct the measurements on the targeted devices a quantification of the introduced error was done. It was found that there are two sources of measurement distortions. One of them is produced as a result of the parasitic reactance, inductance and capacitance, of the setup PCB traces. The second one is produced by the power inductors L_A that are used to power the device and results in parallel with the impedance to measure.

The parasitic PCB traces reactance has been measured by running a test with the system on short and open-circuit to obtain respectively the inductance and the capacitance; the impedance of the power inductors L_A has been measured with a network analyzer. With this data collected, a graph representing the error percentage has been generated. Fig. 4 shows this result.

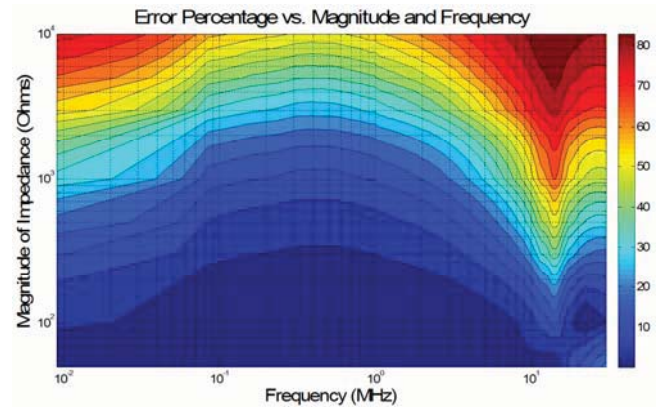


Figure 4. Error percentage as function of Impedance and Frequency.

This graph is here presented as an example of the several error graphs that were constructed depending on circuit configuration. Those are not included in this document for extension reasons.

The abscissa represents frequency spectrum; the ordinate represents magnitude of impedance; and the tone of color represents error percentage according to the color bar on the right of the graph. Red zones indicate higher degree of measurement error while blue zones indicate lower degree of it. Most of the error here encountered is provoked by the decreasing of the power inductors impedance (with frequency) due to parasitic capacitance.

IV. RESULTS

Results obtained with the developed system are very encouraging. Here are presented some of the measurements obtained after a series of tests performed in two automotive windshield wipers motors. In the first device, the internal DC electric engine is separated from its own enclosure as shown in Fig. 5, and it is designated with the name “motor A”.

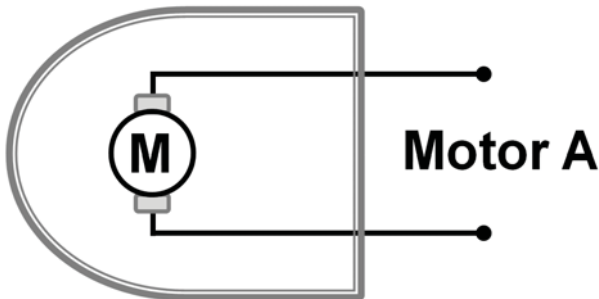


Figure 5. Motor A schematic.

The second windshield wiper includes an EMI filter that makes a direct connection to enclosure as shown in Fig. 6. The values of the capacitor and inductor of the embedded LC filter are 1.5 μF and 10 μH . This load is designated with the name “motor B”

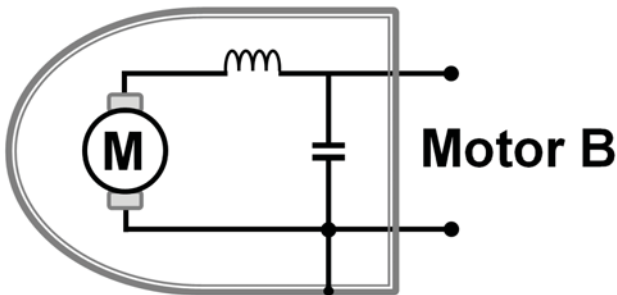


Figure 6. Motor B schematic.

In order to study the behavior of these automotive loads, two kinds of setups are made. The first one consists in comparing the Z_d and Z_C impedances of motor A between powered-on and powered-off states, both with the device located on the ground plane. The second one consists on making a comparison in the motor B Z_C impedance of in powered-on state with the device at certain distance over the ground plane.

As we has mentioned in section II, these results are obtained by means of Z_1 , Z_2 and Z_3 measurements followed by calculations in each case. With the purpose to reducing the measured noise produced by the windshield motor turned-on, an average of five hundred sweeps is performed in each oscilloscope capture.

Fig. 7 shows the differential mode impedance (Z_d) results in motor A, where changes between powered-on and powered-off states can be observed.

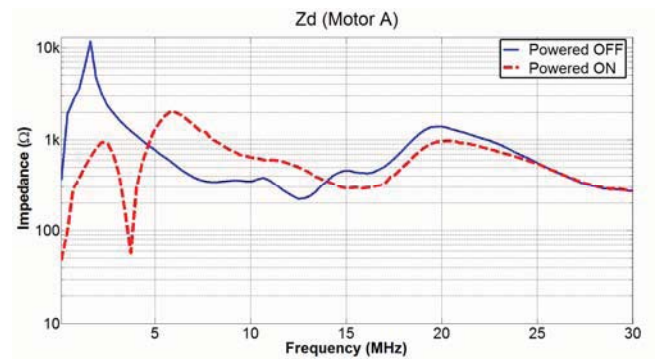


Figure 7. Differential Mode Impedance measurement.

Fig. 8 shows the Z_{C2} (between positive line and ground plane) in motor A results. As we can see on the graph, recorded values also changes if the device is powered-on or powered-off.

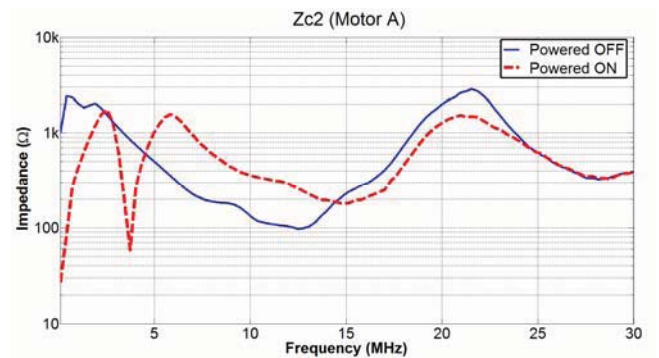


Figure 8. Common Mode Impedance measurement.

Since this measured impedances have to be considered as loads connected to the PLC transmission lines, these kinds of results are very useful when choosing the best frequency range to transmit data in order to minimize the energy required for a correct power line communication.

The next setup is intended to evaluate the effect of the position of the motor B with respect to the ground plane. The value of the common mode impedance is considered when the windshield motor is turned-on. Fig. 9 shows the results of the described setup for Z_{C2} in motor B, where we can observe that an $h=10$ cm separation between DUT and reference ground plane has a significant increase in the common mode impedance above 5 MHz. In that case, it seems that the common mode impedance increases as a result of the parasitic capacitance being diminished with increasing height.

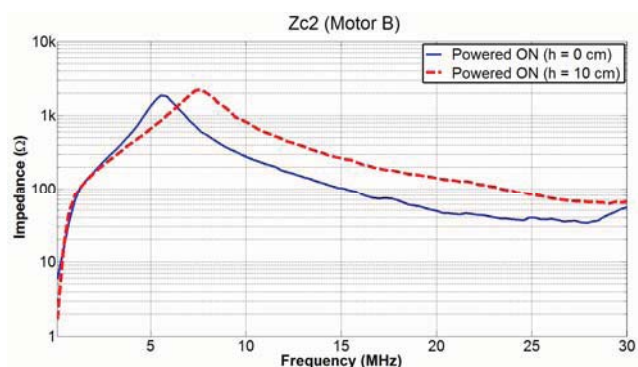


Figure 9. Common Mode Impedance measurement.

Because common mode currents are much more likely to provoke EMI issues than differential mode ones, these kinds of results are useful for PLC systems EMC characterization.

V. CONCLUSIONS

In-vehicle power lines would help to improve vehicle communications systems, without increasing weight, volume or cost of the wiring harness. In this paper, we have provided a measurement system for the electric loads employed in the automotive environment, which will help in the study of the automotive PLC network. Both parameters of impedance, differential mode and common mode have been evaluated, without risk of damage to the instrumentation used. The proposed method allows improving EMI response of the vehicle in the BPL frequency range. Moreover we have measured real examples which have returned satisfactory results. In some of the evaluated loads, like the windshield wiper motor results presented in this paper, it has been found that the distance to the ground plane has a large effect on the common mode impedance. Furthermore, we have obtained the impedance measurement error percentage in our method by running a test with the system on short and open circuit, thus allowing us to quantitatively evaluate the error that is to be expected. Finally, even though this design has been focused the automotive devices, it is also directly applicable in the study of the PLC network in other fields such as aerospace, space and railway.

REFERENCES

[1] N. Navet, Y. Song, F. Simonot-Lion, and C. Wilwert, "Trends in automotive communications systems", *Proc. IEEE*, vol. 93, no. 6, pp. 1204-1223, June 2005.

[2] J. Anatory, N. Theethayi, R. Thottappillil, M. M. Kissaka, and N. H. Mvungi, "The Influence of Load Impedance, Line Length, and Branches on Underground Cable Power-Line Communications (PLC) Systems", *IEEE Transactions on Power Delivery*, vol. 23, no. 1, pp. 180-187, January 2008.

[3] T. Huck, J. Schirmer, and K. Dostert, "Tutorial about the implementation of a vehicular high speed communication system", *IEEE International Symposium on Power Line Communications and Its Applications*, pp. 162- 166, April 2005.

[4] V. Degardin, P. Laly, M. Lienard and P. Degauque, "Impulsive Noise on In-Vehicle Power Lines", *IEEE International Symposium on Power Line Communications and Its Applications*, pp. 222-226, October 2008.

[5] M. Lienard, M. O. Carrion, V. Degardin, and P. Degauque, "Modeling and Analysis of In-Vehicle Power Line Communication Channels", *IEEE Transactions on Vehicular Technology*, vol. 57, no. 2, pp. 670-679, March 2008.

[6] M. Mohammadi, L. Lampe, M. Lok, S. Mirabbasi, M. Mirvakili, R. Rosales, and P. van Veen, "Measurement Study and Transmission for In-vehicle PLC", *IEEE International Symposium on Power Line Communications and Its Applications*, pp.73 – 78, March 2009.

[7] P. Tanguy, F. Nouvel and P. Mazi'ero, "PLC standards for in-vehicle networks", *The 9th International Conference On Intelligent Transport System Telecommunications*, November 2009.

[8] D. Hanse, "The Impact of Power Line Communications", *Compliance Engineering magazine*, 2003.

[9] M. Kitagawa, M. Ohishi, "Measurements of the Radiated Electric Field and the Common Mode Current from the In-house Broadband Power Line Communications in Residential Environment", *IEEE International Symposium on Electromagnetic Compatibility, EMC Europe*, pp. 1-6, September 2008.

[10] Paul, C. R., "Introduction to electromagnetic compatibility," Wiley-Interscience, Second edition, New York, 2006.

[11] A. Perez, A. M. Sanchez, J.R. Regue, M. Ribo, P. Rodriguez-Cepeda, F.J. Pajares, "Characterization of Power-Line Filters and Electronic Equipment for Prediction of Conducted Emissions", *IEEE International Symposium on Electromagnetic Compatibility*, vol. 50, pp. 577-585, September 2008.

[12] ISO 7637-2:2004 - Road vehicles - Electrical disturbances from conduction and coupling -- Part 2: Electrical transient conduction along supply lines only.

[13] A.-M. Sánchez, A. Pérez, J.R. Regué, M. Ribó, P. Rodríguez-Cepeda, F.J. Pajares, "Study of the input impedance variations at power-line terminals of electric and or electronic equipment", *ESA Workshop on Aerospace EMC*, Italy 2009.